Frequency Domain Access Control for Power Line Communications in Home Area Networks

Gautham Prasad, Yinjia Huo, Lutz Lampe, and Victor C. M. Leung
Department of Electrical and Computer Engineering, The University of British Columbia, Vancouver, BC.

***Abstract*—Home area networks (HANs) form the consumer-end installations of a smart-grid communication network. A prominent technology for providing connectivity within a HAN is power line communications (PLC), which equips the network with a readily available communication infrastructure. Broadband PLC (BB-PLC) solutions offer sufficiently high data rates for a multitude of tasks required to be performed in a HAN environment. However, typical BB-PLC networks applying a conventional carrier sense multiple access with collision avoidance (CSMA/CA) medium access control (MAC) protocol, such as that described in the HomePlug Green PHY (HPGP) standard, may collapse in HANs with a large number of users due to poor MAC efficiency. The use of in-band full duplex (IBFD) operation alleviates this network congestion by providing a means to implement CSMA with collision detection (CSMA/CD) to avoid the long collision recovery time. In this paper, we propose methods to further improve the MAC efficiency under a CSMA/CD operation for typical HANs by implementing the priority and contention resolution procedures of the HPGP protocol in the frequency domain. We show through network simulation results that our proposed schemes reduce the time consumed for resolving priorities and contentions by up to 85%.**

I. Introduction and Motivation

Power line communications (PLC) plays a significant role in the last-mile connectivity of a smart grid communication network [1, Ch. 9]. Apart from providing a communication link between smart meters and local access points in a neighborhood area network, PLC is also an attractive technology for communication within a home area network (HAN). Since most appliances in a HAN are already connected to the power line, PLC provides a convenient wired communication medium without any new installations required [2, Ch. 15]. The space for PLC in HANs has historically been occupied by low bandwidth and ultra-low data rate products of X-10, CE Bus, and LonWorks [1, Ch. 7]. However, broadband PLC (BB-PLC) alternatives, such as HomePlug Green PHY (HPGP), offer low-cost low-power solutions while also providing significantly higher data rates, with specifications tailored for smart grid functionalities in HANs [3]. Furthermore, HPGP also provides complete interoperability with other BB-PLC standards, such as HomePlug AV (HPAV), HomePlug AV2 (HPAV2), and IEEE 1901, which are commonly used by indoor high-speed multimedia communication devices [4]. Thereby, HPGP enables a single PLC network for all communication requirements in a HAN [2, Ch. 15].

This work was supported by the Natural Sciences and Engineering Research Council of Canada (NSERC).

The increasing congestion in HANs caused by the growing number of devices connected in a smart-home environment results in the performance degradation of typical HPGP networks. A conventional HPGP-compliant network functions poorly under heavily loaded network conditions as the efficiency of the medium access control (MAC) layer decays rapidly with increasing number of nodes. Prior works have shown that the efficiency could be as low as 10% [5], [6]. One of the reasons for this reduced MAC efficiency is the extended time periods that are lost during frame collisions under a carrier sense multiple access with collision avoidance (CSMA/CA) scheme. A method to reduce this collision recovery time is to implement CSMA with collision detection (CSMA/CD) to immediately terminate transmission in case of a collision. However, CSMA/CD requires the PLC nodes to operate in a full-duplex manner [7, Ch. 5]. The recently developed in-band full-duplex (IBFD) solution for BB-PLC systems has allowed the implementation of CSMA/CD for BB-PLC applications [8]–[11]. Although the collision recovery time is significantly reduced by a CSMA/CD operation, the priority resolution procedure (PRP) and the random back-offs still consume a relatively large time duration during which no data payload is transferred.

In this paper, we aim to further reduce the MAC layer overheads, particularly, the time spent during PRP and back-offs, to increase the MAC efficiency of in-home PLC networks. We propose a solution to implement PRP in the frequency domain by allotting orthogonal frequency bands for each priority levels. Further, we use the same underlying principle to also perform contention resolution in the frequency domain without backing off slot-by-slot as in its time domain counterpart. Concurrently, we use the IBFD operation to simultaneously detect collisions during this period by sensing for other potential frame transmissions. We show through simulation results that our solutions provide a considerable gain in the MAC efficiency for typically encountered HAN traffic conditions.

II. Related Work

Although we find no previous implementations of PRP in the frequency domain, the works in [12], [13] have proposed a solution to apply frequency domain contention resolution for wireless networks. This solution allocates a unique orthogonal frequency division multiplexed (OFDM) sub-carrier to the individual back-off counter (BC) values. During the back-off period, the network nodes transmit a signal on the OFDM sub-carrier mapped to its BC value. In this way, the time during which the BC is counted down to zero is reduced

Fig. 1. Illustration of the initiation procedure of a MAC frame transmission at a node under the conventional HPGP CSMA/CA protocol. (PB: Preamble)

to a single OFDM block duration wherein all nodes are informed of each others BC status. However, apart from the drawback that this limits the range of the possible BC values to the available number of OFDM sub-carriers [14], this scheme may not be effective in BB-PLC systems, since the power line channel consists of multiple deep-notches in the frequency domain [15], [16]. The presence of narrowband noise components on the power line further compromises the effectiveness of this implementation. Therefore, along with presenting a solution that provides a wider frequency band for every BC value to counter the frequency selective nature of the PLC channel, we also propose a method to combat the harsh narrowband noise that could potentially affect the accuracy of detection. Furthermore, we use the IBFD operation during this period to perform contention resolution and collision detection at the same time.

The solution of [12], [13] was further adapted in [17], [18] to reduce the probability of collisions after the frequency domain random back-off. However, such schemes are not applicable to our scenario as we do not wish to alter the procedure in which the BCs are updated by the HPGP protocol. Instead, we apply the CSMA/CD operation that is able to detect and avoid potential frame collisions with minimal overheads [11].

In the following sections, we present our proposed schemes based on frequency domain resolution of the priorities and contentions among network nodes, and demonstrate the effectiveness of our solution through network simulations performed under a realistic smart-home environment with varying HAN traffic conditions.

III. Proposed Schemes

A. Priority Resolution

The conventional CSMA/CA operation adopted by the HPGP standard is shown in Fig. 1. When the channel is sensed idle by the node for a time duration corresponding to the contention inter-frame spacing (CIFS), a frame transmission is initiated starting with the PRP. During the PRP, every node indicates its frame priority as one of the four channel access priority (CAP) levels available in HPGP. The CAPs of all nodes are resolved in two slots in a bit-by-bit manner starting with the most significant bit. A node transmits a priority resolution signal (PRS) to indicate a bit '1', and remains silent otherwise. Each PRS spans seven OFDM blocks, and is sensed at every silent node in the time domain.

To reduce the time spent in PRP, we propose to resolve the CAPs in the frequency domain. The fundamental idea that we use is to divide the available spectrum into four separate frequency bands and map each CAP to an individual sub-band individually to a CAP, so that a two-step bit-by-bit resolution procedure can instead be performed in just one step. We let a node with a priority-p message, i.e., CAPp MAC frame, transmit its PRS only on the pth frequency sub-band. We could further include multiple repetitions as in [19] to guarantee performance under poor channel and noise conditions. At the same time, the node also receives PRSs from all the other active nodes. The node then examines the received PRS spectrum to detect whether a CAP greater than its own has been transmitted. Under conditions when the node does not detect a CAP greater than its own, it wins the PRP and proceeds to the back-off stage. Note that a node is only required to detect a CAP greater than its own, and not required to learn the CAPs of all other network nodes. Although this can, in theory, be achieved in a half-duplex mode, using an IBFD operation to cancel the self-interference (SI) signal provides superior detection accuracy in the presence of closely spaced active sub-carriers in adjacent sub-bands. Furthermore, full-duplex PRP implementation also helps in identifying a contention-free condition where the random back-off procedure could be eliminated when there is a sole PRP winner.

B. Contention Resolution

All the nodes winning the PRP proceed to the back-off stage where they back-off for random durations of time decided by the value of their BC. Network node $n \in \Psi$ selects a random BC value, W_n, drawn from a uniformly distributed random variable in the range $[0, \mathrm{CW}]$, where CW is the contention window size determined by the network protocol, and Ψ is the set of all network nodes that have won the PRP. Since $\mathrm{CW}_{\max} = 63$ for HPGP, this random back-off time can be as long as $63 \times 35.84\ \mu s = 2.25$ ms, which is over 70% longer than even the maximum allowed data frame length [19]. In order to reduce this time duration, we propose to perform back-off in the frequency domain.

1) Advertising BC: We described in Section II that prior works have proposed a frequency domain back-off scheme by transmitting a signal on one particular OFDM sub-carrier based on the chosen W_n [12], [13]. However, such a method suffers from detection errors in BB-PLC, as power line channels are highly frequency selective and experience narrowband noise [15], [16], [20], [21]. To alleviate this problem, we decide to use a larger bandwidth, i.e., a larger number of sub-carriers, to send W_n, such that each node n can advertise its W_n by transmitting a preamble signal on the nth sub-band of carriers reserved for W_n. HPGP generates OFDM preambles using a 384-point inverse fast Fourier transform (FFT), which provides 192 available sub-carriers to transmit on. After permanently notching sub-carriers lying in the amateur radio frequency bands, only 113 of the total sub-carriers are available for data transmission [19]. Therefore, with $\mathrm{CW}_{\max} = 63$, less than two sub-carriers are available to be alloted to represent each W_n. Further, given that the sub-carrier spacing is 195 kHz [19], and that the median coherence bandwidth of BB-PLC channels is about 200 kHz [15], using two sub-carriers is not likely to provide a satisfactory im-

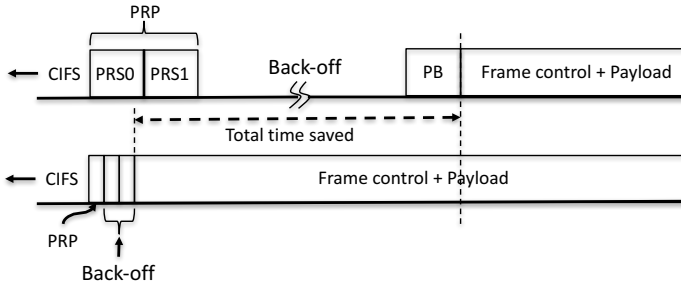

Fig. 2. Illustration of the MAC frame transmission at a node and the time saved using our proposed frequency domain CAP and contention resolution.

provement in detection accuracy. Therefore, to further increase the bandwidth available per W_n, we consider resolving the contentions using two OFDM blocks. We divide the frequency spectrum into ten sub-bands and let the nodes resolve contentions in a digit-by-digit manner starting with the most significant digit (MSD). In the first OFDM-block contention round, all nodes use the IBFD operation to simultaneously transmit and receive the MSD of their W_n. Only the nodes winning the first OFDM-block contention round, i.e., the nodes with the smallest MSD, then proceed to advertise their least significant digit. The nodes that also win the second OFDM-block contention round win the contention resolution procedure. This solution provides each digit of W_n with a bandwidth of over 2 MHz, which is sufficient to compensate for the deep fades in the channel. However, since $\mathrm{CW}_{\max} = 63$ for HPGP, three sub-bands (representing the digits 7, 8, and 9) remain unused while resolving the MSD. To effectively utilize the entire available spectrum, we could further represent W_n in an octal representation and then divide the total bandwidth into eight sub-bands. This provides every octal-digit with a bandwidth of over 2.7 MHz.

The operation of our proposed schemes at a frame transmission initiation is shown in Fig. 2, which also illustrates the amount of time saved by applying our proposed solution. We again highlight that a node only needs to learn the $\min_{\forall n \in \Psi} W_n$, and not W_n of each node, as obtained in [12], [13].

2) Reassigning W_n for Losing Nodes: The node that wins the contention round sets its BC value to zero, and proceeds to transmit the frame control and the data payload. However, the nodes that lose the contention are required to reassign their W_n for the next contention opportunity. Recall that in a conventional time-domain random back-off, the nodes count down W_n to zero, or until it senses a preamble transmission on the line. Thus, every node, m, that loses a contention round eventually assigns

$$W_m \leftarrow W_m - \min_{\substack{\forall n \in \Psi \\ n \neq m}} W_n. \tag{1}$$

With our frequency domain contention resolution procedure, we also apply (1) without counting down in time. Although we do not specifically identify W_n of each node, every listening node is able to deduce $\min_{\substack{n \in \Psi \\ n \neq m}} W_n$ by learning the smallest digit in each of the OFDM-block contention rounds. In this way, we only modify the technique in which the channel access contention is resolved, without altering the algorithm prescribed in the HPGP protocol to determine W_n in the random back-off procedure.

Algorithm 1 Our proposed algorithm at the mth network node.

Start: When message is ready to be transmitted
while sense the channel **do**
if channel is idle for CIFS **then**
  Transmit and receive CAPs
  if $\mathsf{CAP}_m \geq \max_{n \in \Psi} \mathsf{CAP}_n$ **then**
    Pick W_m predetermined from previous round, or
    $W_m \leftarrow U[0, \mathrm{CW}]$
    Transmit W_m, and sense for W_n, $\forall n \in \Psi$, $n \neq m$
    if $W_m < \min_{\substack{\forall n \in \Psi \\ n \neq m}} W_n$ **then**
      Win contention; transmit frame control
    else
      if $W_m = \min_{\substack{\forall n \in \Psi \\ n \neq m}} W_n$ **then**
        Indicate collision; transmit jamming signal
      else
        $W_m \leftarrow W_m - \min_{\substack{\forall n \in \Psi \\ n \neq m}} W_n$
      end if
    end if
  end if
end if

C. Collision Detection

Multiple nodes winning the back-off leads to an eventual frame collision. To avoid data payload collisions and save the associated collision recovery time, we use the IBFD operation during contention resolution to also achieve collision detection. Since the nodes transmit and receive their W_n simultaneously, each such node is informed of at least one other winner when multiple nodes win the second OFDM-block contention round, thereby indicating a future payload collision. Under such a condition, the nodes transmit a jamming signal to inform all the network nodes of a collision. In this way, we use IBFD to combine both contention resolution and collision detection to be performed in the same time slot. The pseudo-code of our proposed protocol is given in Algorithm 1.

D. Signal Detection

A common approach to detect the presence of a signal in a given sub-band is to compare the relative level of the power spectral density (PSD) of the signal with the noise floor. This process is relatively straightforward under additive white Gaussian noise conditions where the signal level can be compared to the noise floor on any silent sub-bands. However, power line noise is colored [20], [21]. It is therefore prudent to pre-compute the noise floor of each sub-band individually. This can be accomplished during the silent periods. Since the PRP begins only after the channel is sensed idle for $\mathsf{CIFS} = 35.84$ μs, the noise floor in each sub-band can

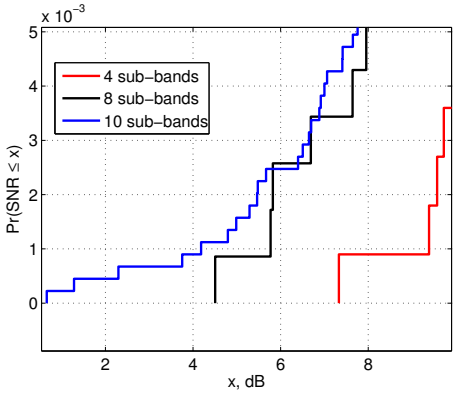

Fig. 3. CDF plot (zoomed) of the average SNR obtained over 1000 randomly generated power line channel and noise conditions.

be computed during this period. Given that our proposed frequency domain PRP and contention resolution completes within $\tau = 30.72$ μs, the noise floor can be assumed to be stationary within this duration of $\mathsf{CIFS} + \tau$.

1) Effect of Narrowband Noise: Most power line environments are subject to narrowband noise whose PSD is typically orders of magnitude larger than the background noise [20], [21]. This increases the probability of missed detection as the narrowband noise increases the computed average noise floor in the affected sub-band. However, measurement results suggest that, on an average, three such narrowband components with a mean bandwidth of less than 450 kHz each, i.e., spanning less than three sub-carriers, are typically present on the power line [21, Table 2]. Therefore, the sub-carriers that are affected by narrowband noise can be easily identified and excluded from the noise floor computation and signal identification during the silent and the resolution periods, respectively.

2) Detection Threshold: Once we compute the average noise floor in each sub-band, we can determine the relative threshold that a signal energy should cross in order to be detected. A low detection threshold increases the probability of false alarms, while a large one increases missed detections. To obtain an empirical indication on the range of possible detection thresholds, we examined the average signal-to-noise ratio (SNR) in each sub-band across 1000 randomly generated power line channel and noise conditions to find the minimum SNR[1]. We divided the available spectrum into four sub-bands for the PRP, and eight sub-bands for the contention resolution. A cumulative distribution function (CDF) plot of the average SNR is shown in Fig. 3. We notice that smaller number of sub-bands (i.e., larger number of sub-carriers in each sub-band) provides a higher minimum SNR as the notches in the channel transfer function are better averaged over greater number of sub-carriers. Fig. 3 also indicates that the probability of encountering low SNR conditions is minimal. Furthermore, the detection threshold can be dynamically assigned for each contention opportunity based on the SNR profile obtained over a previous data payload reception. Hence, for evaluating numerical results in Section IV, we run our simulations with assumption of zero detection errors or false alarms.

3) Detection Errors and False Alarms in Collision Detection: The application of IBFD is indispensable for collision detection as the transmitted and monitored signals occupy the same sub-band. IBFD implemented with an analog interference cancellation solution is shown to be capable of reducing SI to the minimum power line noise floor on idle sub-bands [22]. This ensures that collision detection is devoid of false alarms due to SI. However, SI cancellation could be incomplete in the presence of a received signal [9]. But an incompletely canceled SI can only trigger an alarm and not cause a missed detection. Therefore, a sub-optimal SI cancellation performance does not adversely affect the detection error rate.

E. Discussion on the Implementation

In this final part of Section III, we discuss some salient features of our proposed schemes and possible limitations associated with a practical implementation.

1) Operation in a Heterogeneous HAN: Throughout our analysis in Section III and simulation results we present in Section IV, we consider devices operating with the HPGP protocol. However, a HAN is also expected to consist of PLC devices for high-speed communication purposes, which typically function using the HPAV or IEEE 1901 protocol. HPGP is known to provide complete interoperability with HP1.0, HPAV, HPAV2, and IEEE 1901 BB-PLC standards, and also uses the same PRP and random channel access schemes as them [2, Ch. 15], [19]. Hence, our proposed solutions are not only interoperable with these high throughput BB-PLC standards, but are also applicable to each of these compatible standards in a heterogeneous HAN. We further emphasize that the functioning of the Green PHY preferred allocation and distributed bandwidth control, which guarantee a minimum and maximum time-on-wire for HPGP devices in a hybrid network, respectively [2, Ch. 15], are independent to the operation of our proposed schemes, and can completely coexist with each other.

2) Operation of the Legacy Back-off Procedure: As explained in Section III, our proposed schemes do not alter the procedure in which the back-off, back-off procedural, or the deferral counter is updated for a given network. We only modify the manner in which the CAPs and contentions are resolved. Thus, our schemes can be applied together with other solutions proposed to improve the BC update algorithm, e.g., [5], [6].

3) Hidden Node Collisions: The CSMA/CD scheme used in Section III-C does not address the frame collisions caused due to hidden nodes. However, the IBFD operation could be used by the network nodes as a potential solution to achieve a virtual request-to-send/clear-to-send handshake and eliminate hidden-node collisions [23].

4) Application with Non-IBFD Nodes: Our proposed schemes, without the collision detection procedure, are in

[1]Please refer to Appendices A-A and A-C in [8] for a detailed description on the channel and noise generation procedure and statistics.

principle also implementable on half-duplex devices. However, an uncanceled SI signal is strong enough to potentially saturate the analog-to-digital converter in the receiver. The resulting increase in quantization noise could result in a drastic increase in false alarms. Thus, an IBFD solution with analog interference cancellation, e.g., [9], is most suitable for our application.

5) Extending to Larger $\mathrm{CW}_{\max}$*:* In Section III, we presented a collision resolution procedure for a $\mathrm{CW}_{\max} = 63$. However, extending our solution to larger values of $\mathrm{CW}_{\max}$ is straightforward, either by adding a supplementary OFDM-block contention round, or allocating a smaller bandwidth per W_n by using a higher base representation to denote W_n. The optimal solution then depends on the network conditions.

6) Interleaving Sub-carriers: While allotting different sub-bands for W_n and CAPs in Section III-D, we divided the frequency spectrum into sub-bands that contain contiguous sub-carriers. However, our empirical SNR evaluations indicate that the frequencies below ~ 2 MHz suffer from lower SNRs when compared to higher frequencies. Thus, every CAP and W_n can alternatively be mapped to a different set of sub-carriers each, that spans across the entire frequency spectrum, in order to possibly allow applying a higher detection threshold.

IV. Simulation Results

In this section, we present the network simulation results obtained by using our proposed schemes for a typical indoor PLC HAN.

A. Simulation Settings

We model a heavily loaded indoor PLC network with up to 80 network nodes. To emulate realistic data packets and network node interactions, we run our simulations for varying number of active nodes and different frame lengths.

Since examining MAC efficiency under a saturated network traffic condition is a commonly used metric for the evaluation of the network performance [24], [25], we simulate a network that is saturated with CAP0 MAC frames[2]. However, the inter-arrival time between messages transmitted by devices inside a typical HAN scenario is found to be well emulated by an exponential random distribution [26]–[28]. We thus also generate network traffic in which CAP3 MAC frame arrival follows a Poisson process. Hence, we evaluate the performance of our solutions for two different network traffic scenarios with a common CAP0 MAC frame saturation condition: (a) a saturated network where all active network nodes constantly contend with CAP3 MAC frames, and (b) a comparatively more realistic network in which the higher CAP message arrival follows a Poisson process, where the network nodes contend for the channel with CAP3 MAC frames that have an exponentially distributed random inter-arrival time. In addition, we set the mean inter-arrival times for the CAP3 MAC frames in condition (b) such that they only occupy 50% of the available network resource (time duration), while the rest can be used for CAP0 messages, possible collisions and recovery,

[2]Recall that CAPp MAC frames carry priority-p messages. HPGP has four CAP classes, with $p = 3$ being the highest and $p = 0$ being the lowest CAP.

TABLE I
Simulation Parameters

Parameter	Value
Simulation time (T_{S})	30 s
CIFS	35.84 μs
PRS, preamble, and Back-off slot time (t_{p})	35.84 μs
Frame control length	133.92 μs
Maximum frame length (MaxFL)	1293.64 μs
Extended inter-frame space (EIFS)	1695 μs
t_{OFDM}	5.12 μs
Roll-off interval (at both ends)	$0.5 \times t_{\mathsf{OFDM}}$

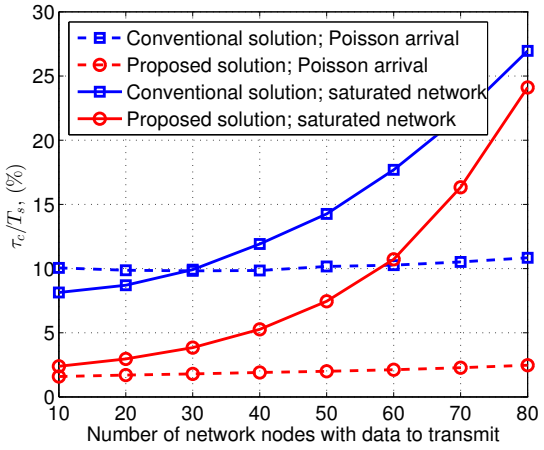

Fig. 4. Percentage of time spent on CAP and contention resolution for varying number of network nodes using the conventional solution and our proposed solution under two different CAP3 network traffic conditions.

and other non data payload transmissions. We tabulate the remaining simulation parameters in Table I, which we obtained from the HPGP protocol [19].

B. Numerical Results

1) Varying Number of Network Nodes: For our first result in Fig. 4, we vary the number of network nodes between 10 and 80 to determine the amount of time, τ_{c}, spent in resolving CAPs and contentions using the conventional approach of [19], and our proposed frequency domain resolution procedure. We fix the transmitted frame length to $t_{\mathsf{FL}} = \mathsf{MaxFL}$ (refer Table I). We observe from Fig. 4 that under a saturated network condition, τ_{c} increases exponentially with the number of nodes due to increased collisions, while τ_{c} remains fairly stable with a Poisson CAP3 message arrival process. In both cases, Fig. 4 shows that τ_{c} is considerably smaller for a frequency domain resolution procedure when compared to its time domain counterpart.

2) Varying Frame Lengths: Our second result shows the variation of the MAC efficiency (η) with t_{FL} in Fig. 5. We vary t_{FL} in 10% steps of MaxFL, and set the total number of active network nodes to 10. We then compute η as (see Table I for parameters)

$$\eta = \frac{t_{\mathsf{FL}}}{\tau_{\mathrm{c}} + \mathsf{EIFS} - \mathsf{MaxFL} + t_{\mathsf{FL}}}. \tag{2}$$

We observe from Fig. 5 that η improves with increase in t_{FL} due to a longer duration of time used for data payload

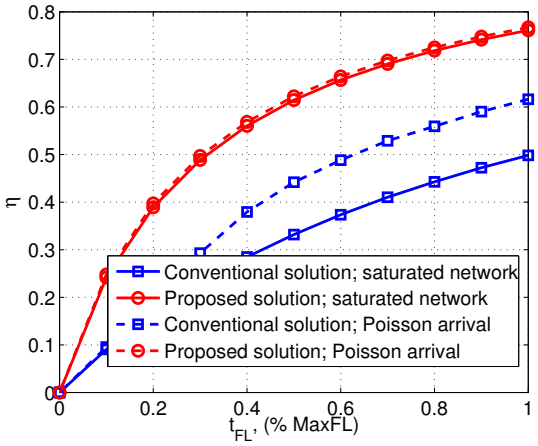

Fig. 5. MAC efficiency versus the data payload frame length using the conventional solution and our proposed solution under different CAP3 network traffic conditions.

transmission. It is noticeable that our solution provides a considerable improvement in η over the time domain resolution procedure. It is also evident from Fig. 5 that a saturated network condition causes larger number of collisions and therefore a smaller η. However, by detecting a collision and immediately terminating the transmission, our solution is seen to be resilient to the effects of collisions, providing a similar η for both traffic conditions.

V. Conclusions

In this paper, we have presented a channel access procedure for BB-PLC systems in which priorities and contentions of the network are resolved in the frequency domain. We have further used the IBFD operation to propose a frequency domain collision detection procedure that achieves a CSMA/CD operation with a reduced collision detection time. The application scenario for such access improved BB-PLC systems are HANs with increased number of devices at the consumer-end as foreseen in the evolution of smart grids. We showed through network simulation results for different HAN traffic conditions and HPGP system parameters that our solutions achieve up to 85% reduction in the time spent on CAP and collision resolution over a conventional time domain approach. We have thereby increased the MAC efficiency of the HPGP protocol to improve its applicability in a heavily loaded smart-home environment.

References

[1] L. Lampe, A. M. Tonello, and T. G. Swart, *Power Line Communications: Principles, Standards and Applications from Multimedia to Smart Grid*, 2nd ed. John Wiley & Sons, 2016.

[2] H. A. Latchman, S. Katar, L. Yonge, and S. Gavette, *Homeplug AV and IEEE 1901: A Handbook for PLC Designers and Users*. Wiley-IEEE Press, 2013.

[3] "HomePlug Green PHY 1.1 White Paper," *Homeplug Powerline Alliance*, Oct. 2012.

[4] S. Galli, H. Latchman, V. Oksman, G. Prasad, and L. Yonge, "Multimedia PLC systems," in *Power Line Communications: Principles, Standards and Applications from Multimedia to Smart Grid*, L. Lampe, A. Tonello, and T. Swart, Eds. John Wiley and Sons Ltd, 2016, ch. 8, pp. 475 – 511.

[5] E. Kriminger and H. A. Latchman, "Markov chain model of homeplug CSMA MAC for determining optimal fixed contention window size," *IEEE Intl. Symp. on Power Line Commun. and Its Appl. (ISPLC)*, 2011.

[6] M. Ayar, H. A. Latchman, and J. McNair, "An adaptive MAC for HomePlug Green PHY PLC to support realistic smart grid applications," in *IEEE Int. Conf. Smart Grid Commun. (SmartGridComm)*, 2015, pp. 587–592.

[7] H. Hrasnica, A. Haidine, and R. Lehnert, *Broadband powerline communications: network design*. John Wiley & Sons, 2005.

[8] G. Prasad, L. Lampe, and S. Shekhar, "In-band full duplex broadband power line communications," *IEEE Trans. Commun.*, vol. 64, no. 9, pp. 3915–3931, Sep. 2016.

[9] ——, "Analog interference cancellation for full-duplex broadband power line communications," in *IEEE Int. Symp. Power Line Commun. and its Appl. (ISPLC)*, Apr. 2017, pp. 1–6.

[10] I. Tsokalo, G. Prasad, S. Mudriievskyi, and R. Lehnert, "CSMA/CD in PLC: Test with full G.hn and IP/UDP protocol stack," in *IEEE Int. Symp. Power Line Commun. and its Appl. (ISPLC)*, Apr. 2017, pp. 1–6.

[11] Y. Huo, G. Prasad, L. Lampe, and V. C. M. Leung, "Mutual preamble detection for full duplex broadband power line communications," in *IEEE Global Commun. Conf. (GLOBECOM)*, Dec. 2016, pp. 1–6.

[12] S. Sen, R. Choudhury, and S. Nelakuditi, "Listen (on the frequency domain) before you talk," in *ACM SIGCOMM Workshop on Hot Topics in Networks*, 2010, pp. 16:1–16:6.

[13] ——, "No time to countdown: Migrating backoff to the frequency domain," in *ACM MOBICOM*, 2011, pp. 241–252.

[14] P. Huang, X. Yang, and L. Xiao, "WiFi-BA: Choosing arbitration over backoff in high speed multicarrier wireless networks," in *IEEE INFOCOM*, 2013, pp. 1375–1383.

[15] F. J. Canete, J. Cortés, L. Díez, and J. T. Entrambasaguas, "A channel model proposal for indoor power line communications," *IEEE Comm. Mag.*, vol. 49, no. 12, pp. 166–174, 2011.

[16] A. M. Tonello and F. Versolatto, "Bottom-up statistical PLC channel modeling—Part I: Random topology model and efficient transfer function computation," *IEEE Trans. Power Del.*, vol. 26, no. 2, pp. 891–898, 2011.

[17] S. A. Alvi and A. Baig, "No more hidden backoff: Advertise backoff in frequency domain," in *IEEE Australasian Telecommun. Netw. and Appl. Conf. (ATNAC)*, 2014, pp. 217–222.

[18] M. Luvisotto, A. Sadeghi, F. Lahouti, S. Vitturi, and M. Zorzi, "RCFD: A frequency-based channel access scheme for full-duplex wireless networks," in *IEEE Int. Conf. Commun. (ICC)*, 2016, pp. 1–7.

[19] "HomePlug Green PHY specification release," *HomePlug Powerline Alliance*, pp. 1 – 736, 2013.

[20] J. A. Cortés, L. Díez, F. J. Cañete, and J. J. Sánchez-Martínez, "Analysis of the indoor broadband power-line noise scenario," *IEEE Trans. Electromagn. Compat.*, vol. 52, no. 4, pp. 849–858, 2010.

[21] D. Benyoucef, "A new statistical model of the noise power density spectrum for powerline communication," in *Intl. Symp. Power Line Commun. and its Applications (ISPLC)*, 2003, pp. 136–141.

[22] G. Prasad and L. Lampe, "Full-duplex spectrum sensing for broadband power line communications," in *IEEE Intl. Symp. Power Line Commun. and its Appl. (ISPLC)*, Apr. 2017.

[23] J. I. Choi, M. Jain *et al.*, "Achieving single channel, full duplex wireless communication," in *ACM MOBICOM*, 2010, pp. 1–12.

[24] G. Bianchi, "Performance analysis of the IEEE 802.11 distributed coordination function," *IEEE J. Sel. Areas of Commun.*, pp. 535–547, Mar. 2000.

[25] F. Inoue, M. Morikura, T. Nishio, K. Yamamoto, F. Nuno, and T. Sugiyama, "Novel coexistence scheme between wireless sensor network and wireless LAN for HEMS," in *IEEE Int. Conf. Smart Grid Commun. (SmartGridComm)*, Oct 2013, pp. 271–276.

[26] Y.-J. Lin, H. A. Latchman, M. Lee, and S. Katar, "A power line communication network infrastructure for the smart home," *IEEE Wireless Communications*, vol. 9, no. 6, pp. 104–111, 2002.

[27] M. Laner, P. Svoboda, N. Nikaein, and M. Rupp, "Traffic models for machine type communications," in *Int. Symp. on Wireless Commun. Sys. (ISWCS)*. VDE, 2013, pp. 1–5.

[28] S. W. Lai, G. G. Messier, H. Zareipour, and C. H. Wai, "Wireless network performance for residential demand-side participation," in *IEEE PES Innovative Smart Grid Techn. Conf.*, Oct 2010, pp. 1–4.